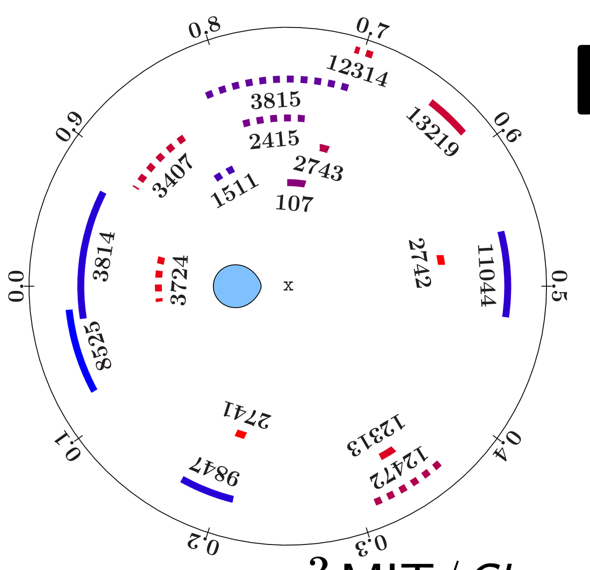

Feeding the Monster: Wind Accretion in Cygnus X-1

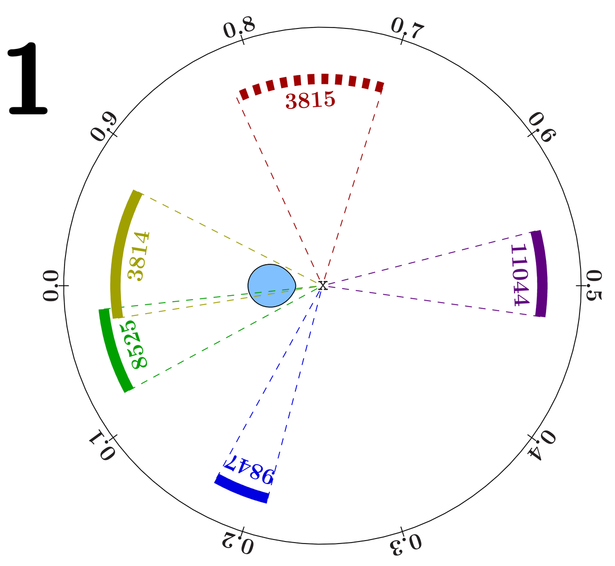

Ivica Miškovičová[1], Natalie Hell[1,4], Manfred Hanke[1],
{Ivica.Miskovicova, Natalie.Hell}@sternwarte.uni-erlangen.de
M. A. Nowak[2], K. Pottschmidt[3], N. S. Schulz[2],
V. Grinberg[1], T. Dauser[1], R. Duro[1], G. V. Brown[4] and J. Wilms[1]

[1] Remeis-Observatory/ECAP, University of Erlangen-Nuremberg, Germany
[2] MIT/*Chandra* X-ray Center, Cambridge (MA), USA [3] CRESST-UMBC/NASA-GSFC, Greenbelt (MD), USA [4] LLNL, Livermore (CA), USA

Abstract

The accretion onto the black hole in the HMXB Cygnus X-1 is powered by the strong line-driven wind of its O type companion HDE226868. The wind is highly structured: clumps of lower ionization stages and temperatures, originating from large density and temperature inhomogeneities, are embedded in highly photoionized material. Due to the strong tidal interactions in the system, the wind is focused along the binary axis, resulting in its variations over the orbital phase.
We present results of the detailed analysis of the stellar wind in the hard state of Cygnus X-1 from high-resolution Chandra-HETGS observations at four distinct orbital phases: $\phi \sim 0$, ~ 0.2, ~ 0.5 and ~ 0.75. All light curves but the one at $\phi \sim 0.5$ show strong absorption dips that are believed to be caused by the clumps in the wind. We compare the spectral properties of dips and persistent flux: while the H-like and He-like absorption lines reveal the highly photoionized wind, the lines of lower ionization stages visible only in the dip spectra constrain the properties of the clumps. Comparison between different orbital phases allows us to study the complex structure and dynamics of the wind.

Chandra's view of Cyg X-1: Hard vs. soft state

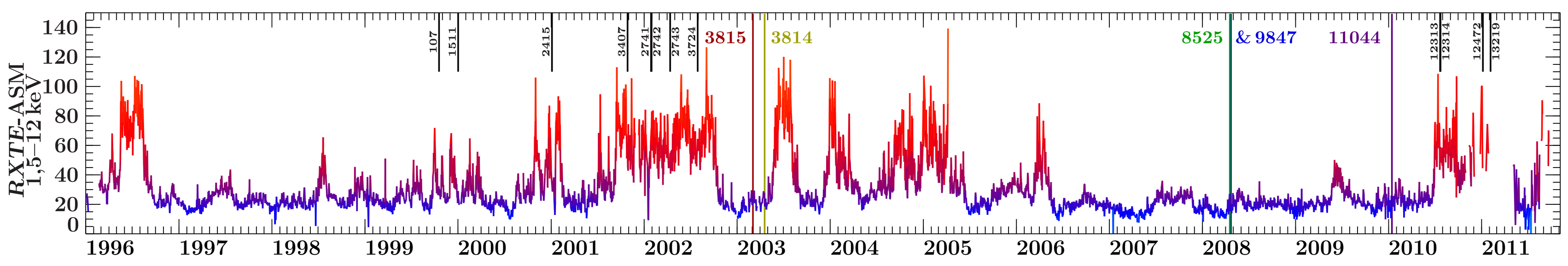

Cyg X-1 is a nearby ($1.86^{+0.12}_{-0.11}$ kpc; Reid et al. 2011), bright (~300mCrab in the ASM band in hard state), and persistent source. The 1.5–12 keV *RXTE*-ASM light curve shows transitions between low/hard and high/soft state[a]. To study the stellar wind, **the low/hard or lower intermediate state are essential**. In the soft state, the source is bright enough in the UV and the soft X-rays to fully photoionize the stellar wind. Consequently, the wind is suppressed because the radiative driving force of the UV photons from the donor star is reduced as the ionized gas is transparent for UV radiation. All *Chandra* observations prior 2012 are shown. (Title left: their distribution over orbital phase $\phi_{\rm orb}$.). Black lines indicate soft state observations. Five observations caught **Cyg X-1 in the hard state** (<40 cps in ASM) and were chosen for our analysis: ObsIDs 3815, 3814, 8525 & 9847 and 11044.

[a] For a detailed spectral and timing analysis see Grinberg et al. (2012), in prep.

Chandra's view of Cyg X-1: $\phi_{\rm orb} \sim$ 0.75, 0.95, 0.05, 0.2, and 0.5

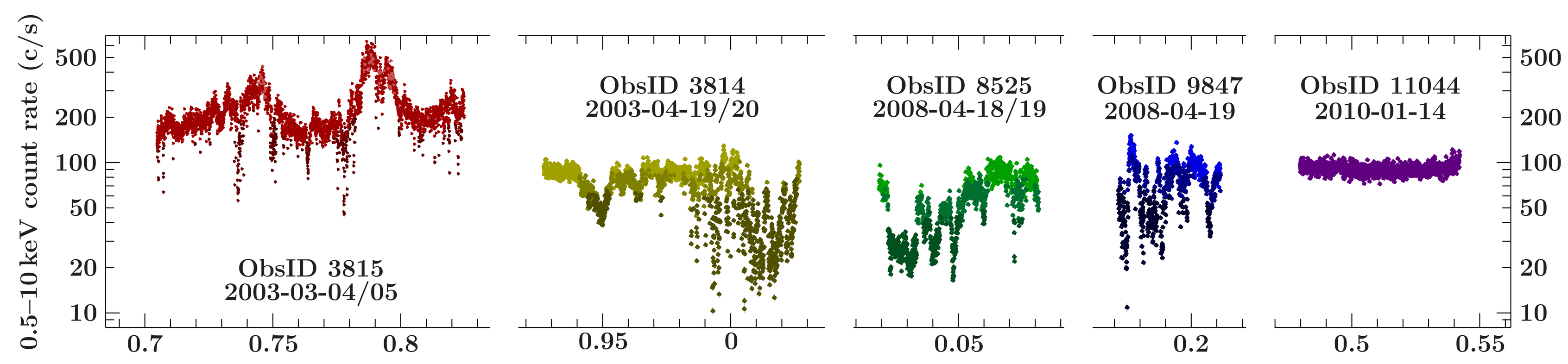

Orbital phase ϕ (At ϕ=0, Cyg X-1 is only seen through the densest part of the donor's stellar wind.)

Analyzing observations at phases $\phi_{\rm orb} \sim 0.75$, 0.95, 0.05, 0.2, and 0.5 enables us to **probe all prominent parts of the wind of Cyg X-1**. The light curves at $\phi_{\rm orb}{\sim}0$ are shaped by violent **absorption dips**, but dipping occurs already at $\phi_{\rm orb}{\sim}0.75$ and has not ceased at $\phi_{\rm orb}{\sim}0.2$, though the dip events seem to become shorter and weaker with distance from $\phi_{\rm orb}{\sim}0$, until the ObsID 11044 at $\phi_{\rm orb}{\sim}0.5$ is totally **free of dips**. Different stages of dipping (as color-coded) correspond to the **hot, ionized wind** (**non-dip** level), and **clumps** (**dips**), and are, therefore, analyzed separately.

Non-dip Spectra: Modulations with orbital phase

Line Profiles

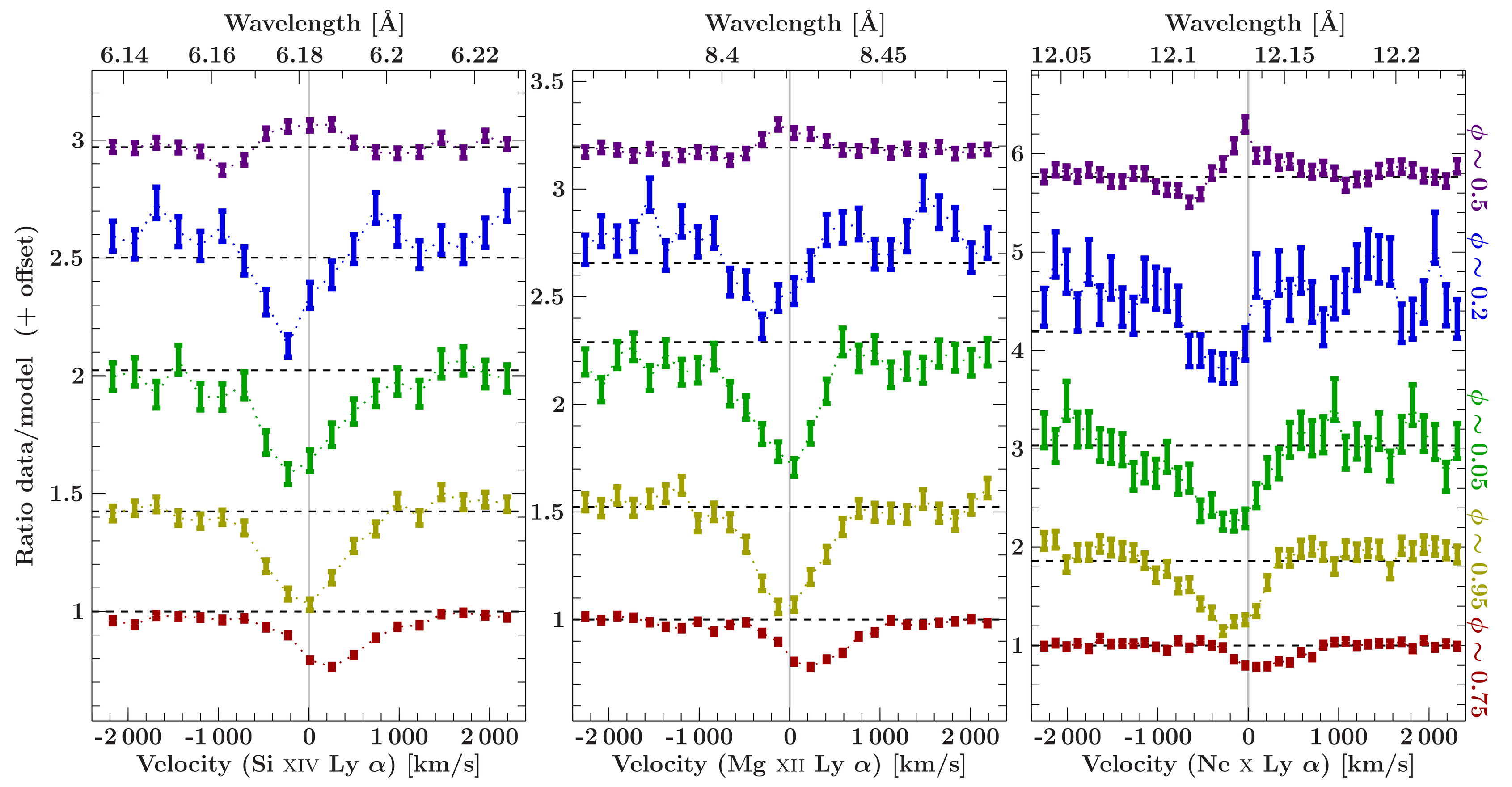

The **highly photoionized wind** is detected via numerous **H- and He-like absorption lines**. Their profiles change over the orbital phase. As an example we show Si XIV, Mg XII, and Ne X. Lines at $\phi_{\rm orb}{\sim}0.75$ are observed in absorption, redshifted by 100–400 km s^{-1} (Miškovičová et al. 2011). Stronger absorption lines with small blueshift ($\lesssim$200 km s^{-1}, Hanke et al. 2009) are observed around $\phi_{\rm orb}{\sim}0$ and ~ 0.2. We detect **clear P Cygni profiles** – for the **first time for Cyg X-1** – at $\phi_{\rm orb}{\sim}0.5$ (Miškovičová et al. 2011). The velocity shifts of the *strong emission* components are consistent with zero, while the *weak absorption* tails show high blueshift (~500–1 000 km s^{-1}), which is a direct proof that a **non-focused part of the wind exists also on the X-ray irradiated side of the donor star** and is accelerated to high velocities. The weakness of the absorption lines suggests that the wind is less dense at $\phi_{\rm orb}{\sim}0.5$ than at $\phi_{\rm orb}{\sim}0$. No emission is seen at $\phi_{\rm orb}{\sim}0$, thus, any emitting gas must be at small projected velocity, such that the emission fills only part of the observed absorption. The gas is also seen at low velocity at $\phi_{\rm orb}{\sim}0.5$. If we observe the same wind structure, only seen at different angles, than its full space velocity must be small, related, e.g. to the focused wind. Proper P Cygni profiles fitting and further observations at yet uncovered orbital phases should bring more understanding of this question.

Dip Spectra: Low Ionization stages

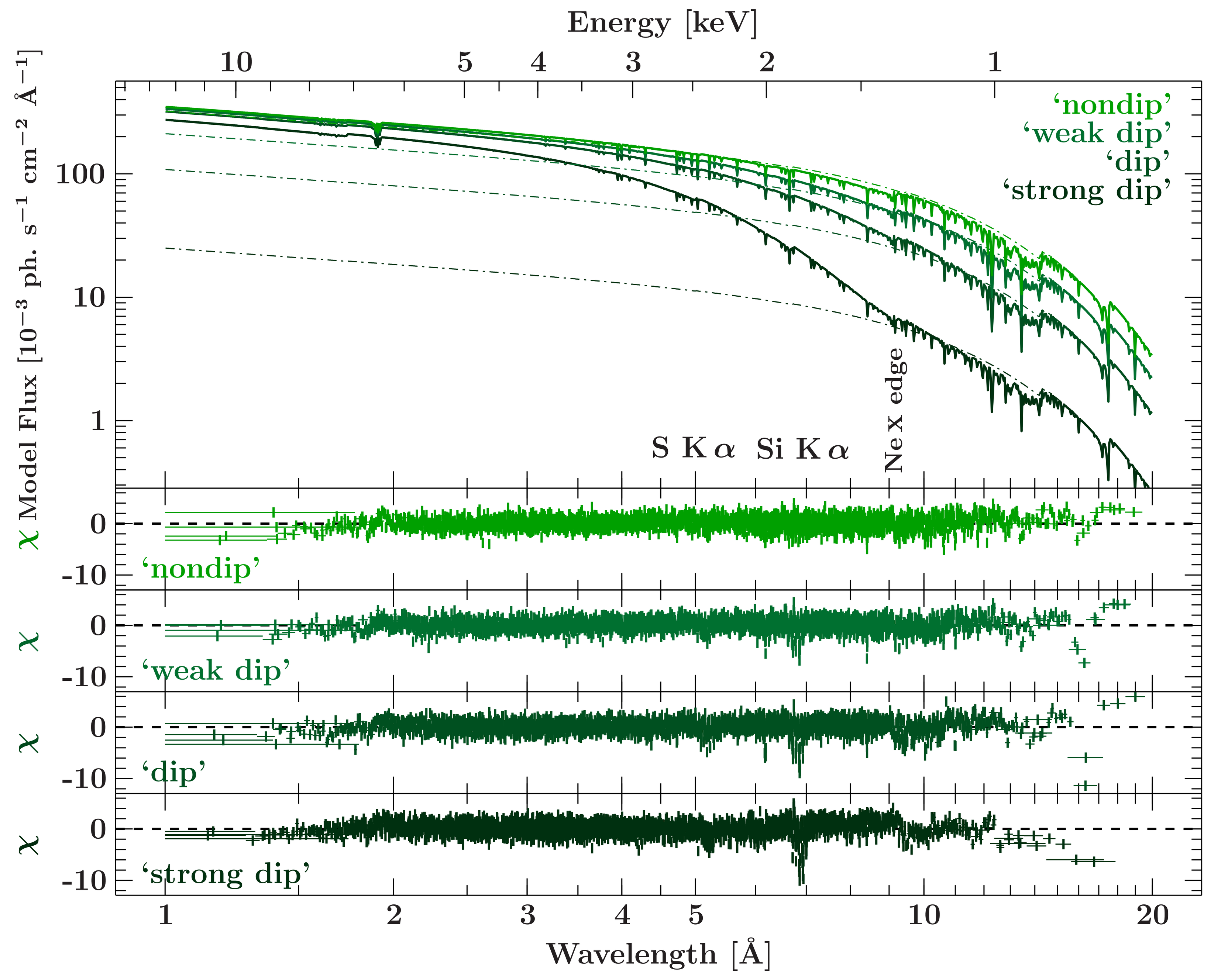

ObsID 8525 is the observation with the **strongest dips**, therefore it was split into four parts according to the stage of dipping. The spectrum hardens and the **flux is reduced during the dips**. While absorption lines of Si XIV and Si XIII are already present in the non-dip spectrum, the dip spectra contain **additional strong absorption lines** that can be identified with Kα transitions of **lower ionized Si** XII–VII. Also Kα transitions of **lower ionized S** are visible, but the lines are generaly weaker than Si.

Velocity shifts & Column densities

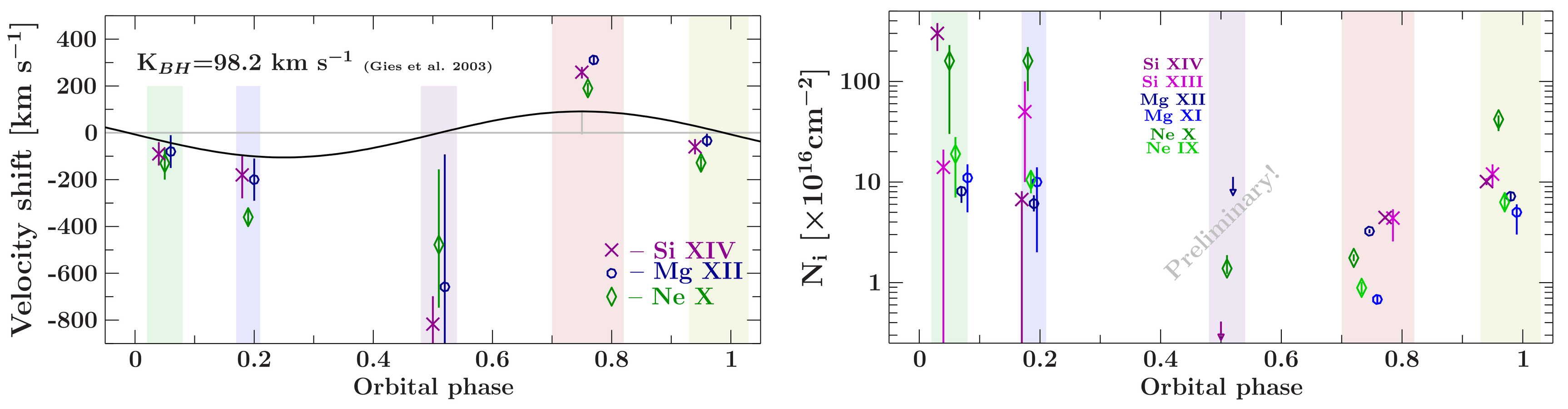

Velocity shift and column density evolution can be directly compared for ObsIDs 3815, 3814, 8525 and 9847 as they show similar behaviour. When we compare these values with ObsID 11044, we have to take into account that this spectrum contains P Cygni profiles that change the behavior of the parameters. We again compare Si XIV, Mg XII, and Ne X. (For column density also He-like lines: Si XIII, Mg XI, and Ne IX, when possible.) **Velocity shifts** are rather low and follow the radial velocity of the black hole (black sine curve), which suggests that **we probe material infalling onto the black hole**. We know that there is an $N_{\rm H}$ variation over orbital phase seen in Cyg X-1 (Grinberg et al. 2012, in prep.), having maximum at $\phi_{\rm orb} \sim 0$, in the focused wind beam, and minimum on the other side at $\phi_{\rm orb} \sim 0.5$. Despite the large errorbars in ObsIDs 8525 and 9847 (because of low statistics), the column densities N_i of investigated elements show similar trend, as expected.

Electron Beam Ion Trap (EBIT) measurement

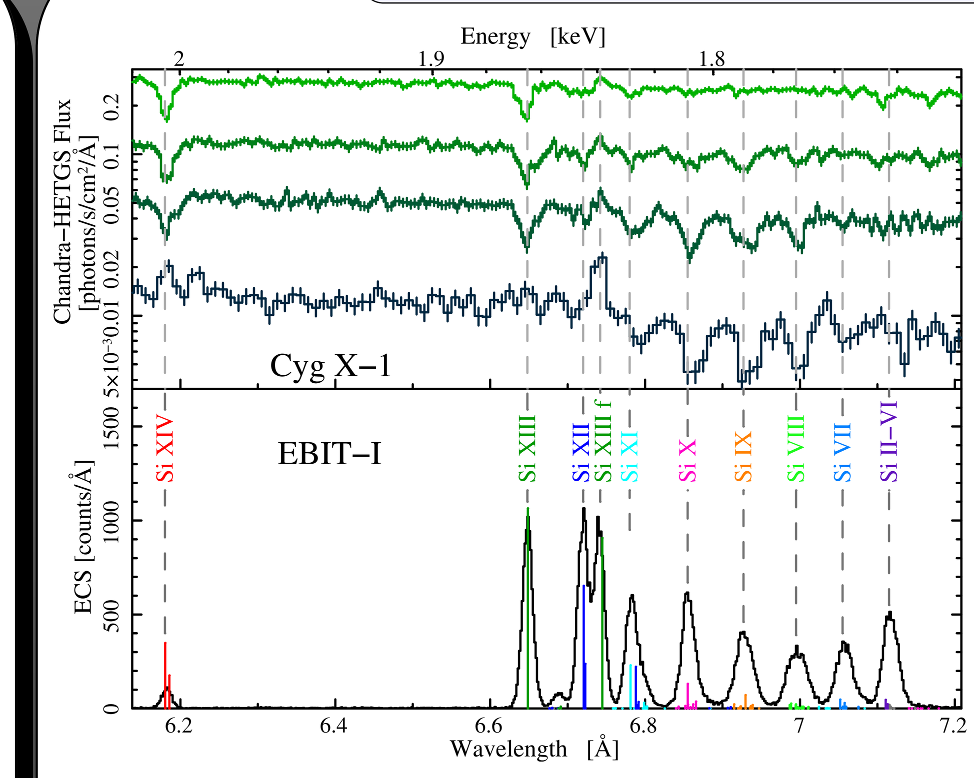

The upper panel zooms onto the **Si region** of ObsID 8525. Absorption lines of lower ionization states of Si (and S) appear and become stronger with increasing dipping, while lines originating from the highly charged ions become weaker until they almost vanish during the deepest dips. The uncertainty of theoretically calculated rest-wavelengths for these lines is of the order of the expected line shifts. Our laboratory measurements with the Lawrence Livermore National Laboratory EBIT-I and the EBIT Calorimeter Spectrometer (ECS; lower panel) allow us to derive the Doppler shifts more accurately. We find **shifts consistent with zero velocity of the absorber throughout all ionization states in all dipping stages** of this observation, providing **evidence for the absorbing material being embedded in the highly ionized wind** as clumps with an onion-like ion structure.

Black Hole Universe — Friedrich-Alexander-Universität Erlangen-Nürnberg — ecap Erlangen Centre for Astroparticle Physics

We acknowledge funding from the EU under grant agreement number ITN 215212 "Black Hole Universe" and by BMBF under DLR grant 50 OR 1113. This work was partially completed by LLNL under Contract DE-AC52-07NA27344, and is supported by NASA grants to LLNL and NASA/GSFC.

References

Grinberg, V., Böck, M., & Pottschmidt, K. 2012, in prep.
Hanke, M., Wilms, J., Nowak, M. A., et al. 2009, , 690, 330
Miškovičová, I., Hanke, M., Wilms, J., et al. 2011, Acta Polytechnica, 51, 85
Reid, M. J., McClintock, J. E., Narayan, R., et al. 2011, , 742, 83